DFTT 14/96
NORDITA 96/25-P
April, 1996

# QCD corrections to the production of a heavy quark pair plus a hard photon in $e^+e^-$ annihilation

**Lorenzo Magnea**[1]
*NORDITA*
*Blegdamsvej 17, DK-2100 Copenhagen Ø, Denmark*

**Ezio Maina**[2]
*Dipartimento di Fisica Teorica, Università di Torino*
*Via P. Giuria 1, I-10125 Turin, Italy*
*and INFN, Sezione di Torino*

**Abstract**

We present complete results for the $O(\alpha_s)$ corrections to the production of a heavy quark pair plus a hard photon, in $e^+e^-$ annihilation, including both photon and $Z$ intermediate states. Virtual corrections are calculated analytically in $4-2\epsilon$ dimensions, together with the soft approximation to the real emission diagrams. After cancellation of infrared divergences, real and virtual contributions are combined numerically to obtain the cross section for the production of two heavy quark jets plus a hard photon in next-to-leading order. The resulting fully differential cross section can be used to construct arbitrary distributions with the desired experimental cuts.

[1]On leave from Università di Torino, Italy
[2]e-mail: maina@to.infn.it

# 1 Introduction

Out of several millions of $Z$ bosons produced by LEP1, several tens of thousands decayed into heavy quark pairs. This provides enough statistics to compare theory and experiment beyond leading order, and possibly to isolate quark mass effects in the radiative corrections. On the other hand, the measured partial widths of the $Z$ to $c$ and $b$ quarks, $\Gamma_c$ and $\Gamma_b$, differ by a few standard deviations from the predictions of the Standard Model (SM) [1], and provide the most significant discrepancy between high precision data and the otherwise spectacularly successfull SM. This ensures that all aspects of heavy flavour production will be actively studied also in the future. Finally, quark mass corrections are going to be extremely important at any of the next-generation $e^+e^-$ colliders that are currently being planned, where top quark pairs are going to be abundantly produced, while the top quark mass will be a significant fraction of the center of mass energy. At leading order it has been shown that quark masses substantially affect three, four and five jet cross sections [2, 3]. However, NLO calculations for heavy quark production in $e^+e^-$ annihilation are available only for a two-particle final state [4]. With the present paper, we begin an analysis of heavy quark production processes in $e^+e^-$ annihilation with more than two particles in the final state, at next-to-leading order in QCD. Here we present results for the production of two heavy quark jets plus a hard photon, at $O(\alpha^3\alpha_s)$. While, as we shall see, this process is of interest for several reasons, the calculation can also be considered as a preliminary step towards the complete evaluation of the 3-jet production process at $O(\alpha^2\alpha_s^2)$, with massive quarks. We are thus interested in the mass corrections to the results of Ref. [5], and in perspective to the results of Ref. [6].

The importance of studying events with hard photons and hadrons in the final state, in $e^+e^-$ collisions, has been emphasized by many authors [7]. In particular, it has been argued that photon radiation can be used for a relatively clean determination of the weak couplings of the radiating quark [8]. Further, photon production is expected to give signals of several new physics processes, including Higgs production [9], both in the Standard Model and in its supersymmetric extension, and exotic decays of heavy quarks [10]. A full understanding of QCD corrections to the standard production process is however essential in all these cases. Here we will concentrate on just these corrections, in the case in which the mass of the quarks is not negligible.

The analysis of hard photon events, and in particular of events with isolated photons, with which the present work is concerned, is complicated both theoretically and experimentally by the necessity to impose cuts to define the event and to avoid the soft singularities of perturbative calculations. The difficulties arising were thoroughly discussed, in the case of massless quarks, in Refs. [11], [12] and [13]. Experimental results on the production of hard isolated photon at Lep can be found in Ref. [14] and references therein. The case of massive quarks is somewhat different, and in fact simpler, because the quark mass regulates the collinear photon-

quark and gluon-quark divergences, which are softened to logarithms of the quark mass; only the infrared divergences associated with soft emission remain to be dealt with. While in Ref. [11] it was argued that a genuine non-perturbative contribution survives even for isolated photons, signalled by the collinear divergence associated with photon emission, which must be reabsorbed in a non-perturbative photon fragmentation function, in the case at hand a large quark mass acts as a natural cutoff for non-perturbative effects. A partial breakdown of perturbation theory is signalled only by the appearance of potentially large logarithms of the quark mass, which may eventually be resummed. It was also argued in Ref. [15] that isolated photon cross sections suffer from a failure of the usual factorization theorem. However such a failure takes place only at the boundary of phase space, and does not significantly affect our results.

We now proceed to describe how we deal with photon isolation and with the cancellation of infrared divergences. Next we will describe briefly the steps involved in the calculation of the various contributions to the cross section. In Sec. 3 we will deal with the virtual corrections, which constitute the bulk of the analytic calculations and we will briefly describe the real emission contributions. In Sec. 4 we will give our results.

# 2 Photon isolation and cancellation of infrared divergences

As with all NLO calculations, to obtain a finite answer for a process with $p$ partons in the final state, it is necessary to combine the virtual one-loop corrections to the production of $p$ partons with the tree-level contributions having $p+1$ partons in the final state, integrated over the singular regions of phase space. The exclusive production of a photon in the final state is not, as a consequence, an infrared safe process, since diagrams in which the photon is virtual are excluded. It is then necessary, both theoretically and experimentally, to introduce a cut in photon energy, $E_{min}$, to exclude infrared photons. In a hadronic environment, with hadrons clustered into jets, it is further desirable to isolate the photon from hadronic jets. This makes for a cleaner experimental definition of the event, while from a theoretical point of view it excludes the regions corresponding to collinear emission, in which perturbation theory fails or becomes unreliable. This angular isolation is the source of most of the ambiguities studied in [11, 12, 13], since perfect isolation cannot be achieved either theoretically or experimentally, and it is necessary to clarify the interplay of the cuts with the jet reconstruction algorithms. Let us first explain in some detail the handling of infrared divergences associated with the gluon, then we will introduce the auxiliary cuts needed for photon isolation.

For the cancellation of infrared divergences, we use here a simplified version of the "subtraction method" described in Ref. [16]. We have also tested the "phase space slicing method" of Ref. [17], and the results of the two methods are fully com-

patible. Our procedure can be summarized as follows. Let $d\sigma_1^{(3)}$ be the differential cross section for the production of a heavy quark-antiquark pair plus a hard photon, at one loop in QCD, and let $d\sigma_0^{(4)}$ be the tree-level differential cross section for the production of the same final state with an extra gluon. Both cross sections are singular, due to the infrared divergence associated with the extra gluon, while in this case there are no collinear divergences, since they are cut off by the quark mass. In both cases, the singular contributions can be isolated and computed analytically in $4-2\epsilon$ dimensions. Let us denote these singular contributions by $d\sigma_{1,soft}^{(3)}$ and $d\sigma_{0,eik}^{(4)}$, respectively. Both are proportional to the Born cross section for the 3-particle final state, $d\sigma_0^{(3)}$. If we now integrate $d\sigma_{0,eik}^{(4)}$ over the soft gluon phase space (defined for example by a cutoff in the quark-gluon invariant mass, or in the gluon energy in a suitable frame, which we denote here by $\Delta$) the result, $d\sigma_0^{(4\to3)}(\Delta)$, will cancel the IR singularity of $d\sigma_{1,soft}^{(3)}$, by the Bloch-Nordsieck mechanism. We can thus define a finite NLO cross section for the production of two heavy quark jets plus a hard photon as

$$d\sigma_1^{(2jets+\gamma)} = \left[d\sigma_1^{(3)} + d\sigma_0^{(4\to3)}(\Delta)\right] + \left[\int_R d\sigma_0^{(4)} - \int_\Delta d\sigma_{0,eik}^{(4)}\right] \quad . \tag{1}$$

Here the first bracket is finite by the Block-Nordsieck mechanism, while the second one is finite by construction. $R$ is the region in phase space in which the soft gluon is not experimentally detectable, and it is unrelated with the parameter $\Delta$ introduced before. The first bracket can be computed analytically in $4-2\epsilon$ dimensions up to the point where the cancellation of divergences can be explicitely checked. The resulting finite expression can then be computed numerically. The second bracket, being finite in four dimensions, can be evaluated numerically directly in $d=4$ using a numerical integration program. This is important in this case since the exact expression for $d\sigma_0^{(4)}$ is long and cumbersome. Notice that no approximations have been introduced in Eq. 1, since exactly the same term was added and subtracted.

So far only the cutoff $\Delta$ has been introduced, which defines the border of the soft gluon region. Next, we need to restrict the photon phase space to define an isolated photon cross section, without spoiling the cancellation outlined above. This we do as follows. First of all, we introduce energy and transverse momentum cuts to exclude soft photons and photons lost in the beam pipe. The second of these cuts is also necessary to avoid the collinear divergence associated with collinear photon emission from the massless lepton lines in the initial state. Thus events with photons having an energy $E_\gamma < E_{min}$ or a transverse momentum $p_\gamma^T < p_{min}^T$ in the center of mass frame are rejected. Next, at the parton level, we impose a cut $\theta_{min}$ on the angle between the photon and either the quark or the antiquark. An event is rejected if the photon is too close to them. The gluon is treated differently; soft gluons must be integrated over full phase space to cancel the infrared divergences of the virtual correction, so we must allow soft gluons to be emitted in the vicinity of the photon. This is achieved by introducing an auxiliary infrared cutoff $\Delta_0 < \Delta$ on, say, the quark-gluon invariant mass $m_{Qg}$. Then for gluons such that $m_{Qg} < \Delta_0$ no

isolation cut is imposed, whereas gluons with $m_{Qg} > \Delta_0$ are not allowed inside the isolation cone of the photon. We remark that treating quarks and gluons differently is quite natural in the case of massive quarks since these can in principle be tagged. At the parton level this defines a cross section for the production of a hard isolated photon in association with up to three partons, with a finite amount of partonic energy allowed inside the isolation cone. The events that have passed the cuts are then fed through a jet reconstruction algorithm, say Jade, or Durham, where only the partons, but not the photon, are recombined into jets. Finally, we test if the isolation of the photon has survived jet reconstruction, using the same separation parameter $y_{cut}$ for the definition of the number of jets and for photon isolation. It may happen in fact that two soft partons that were outside the photon isolation cone are recombined by the jet algorithm into a jet whose axis lies inside the cone. Such events do not correspond to the experimental definition of an isolated hard photon, and are again discarded.

Summarizing, our definition of the isolated photon cross section depends on five phase space cuts, $E_{min}$, $p_{min}^T$, $\theta_{min}$, $\Delta$ and $\Delta_0$. Consistency demands that our results be independent of the definition of the soft gluon region, so they should be stable against variations of the infrared cutoffs $\Delta$ and $\Delta_0$. As explained in more detail in section 4, we have verified that this is indeed the case.

# 3 Outline of the calculation

The handling of virtual corrections is straightforward, if lengthy. Since the masses of the heavy quarks are comparatively well known, we choose on-shell renormalization for the quark mass and wave function. As a consequence, quark self-energies on the external legs do not contribute, except for the fact that an infrared divergence is introduced in the quark wavefunction renormalization, which will cancel when combined with real gluon emission, as in QED. The strong coupling is not renormalized, since the corrections computed here are leading order in $\alpha_s$.

To fix our notations and normalizations, let us start by displaying the structure of the relevant matrix element. We consider the reaction

$$e^-(p) + e^+(p') \to Q(p_1) + \bar{Q}(p_2) + \gamma(p_3) \quad , \tag{2}$$

where $Q$ is a quark of mass $m >> \Lambda_{QCD}$, *i. e.* a $c$, $b$ or $t$ quark. Including photon emission from the initial state leptons, the matrix element for the reaction in Eq. (2) can be written as

$$\begin{aligned} M(p_1,p_2,p_3;s,\mu) &= \frac{1}{s}\left(L_\mu^{(0)}(\gamma)H_{(1)}^\mu(\gamma) + L_\mu^{(1)}(\gamma)H_{(0)}^\mu(\gamma)\right) \\ &+ \frac{1}{s - M_Z^2 + \mathrm{i}\Gamma_Z M_Z}\left(L_\mu^{(0)}(Z)H_{(1)}^\mu(Z) + L_\mu^{(1)}(Z)H_{(0)}^\mu(Z)\right) \quad . \end{aligned} \tag{3}$$

Here $L_\mu^{(i)}(V)$ is the leptonic vertex for the production of vector boson $V$, including real photon radiation if $i = 1$, while $H_\mu^{(i)}(V)$ is the corresponding hadronic vertex.

Specifically,

$$\begin{aligned} L_\mu^{(0)}(\gamma) &= -\mathrm{i}\; e\; \bar{u}_e(p)\gamma_\mu v_e(p') \\ L_\mu^{(0)}(Z) &= -\mathrm{i}\; \frac{e}{2\sin\theta_W\cos\theta_W}\; \bar{u}_e(p)\gamma_\mu \left(c_V^e - c_A^e\gamma_5\right) v_e(p') \quad , \end{aligned} \tag{4}$$

where the electron couplings to the $Z$ boson are given by

$$c_V^e = -\frac{1}{2} + 2\sin^2\theta_W \quad , \qquad c_A^e = -\frac{1}{2} \quad . \tag{5}$$

Initial state photon radiation is contained in $L_\mu^{(1)}(V)$, which is the sum of the two diagrams obtained by inserting a photon on either of the leptonic legs in Eq. (4). Similarly we can write

$$H_\mu^{(i)}(V) = H_\mu^{(i,0)}(V) + \alpha_s H_\mu^{(i,1)}(V) \quad . \tag{6}$$

Here the tree level contributions $H_\mu^{(0,0)}(\gamma)$ and $H_\mu^{(0,0)}(Z)$ are obtained from Eq. (4) by replacing the electron couplings to the various currents with the corresponding quark couplings. Final-state tree-level photon emission is contained in $H_\mu^{(1,0)}(V)$, which is again the sum of two diagrams for each gauge boson. $H_\mu^{(0,1)}(V)$ is the QCD radiative correction to $Q\bar{Q}$ production, and, since we are using on-shell renormalization for the quark lines, it includes only the vertex correction diagram. Finally, the bulk of the computation is devoted to $H_\mu^{(1,1)}(V)$, the QCD correction to photon emission from the final state quark lines. Not counting quark self-energies on external legs, this correction comprises eight diagrams, two of which are of "box" type.

The first step in the analysis of the hadronic vertex is a Passarino-Veltman decomposition [18] of the tensor integrals contained in $H_\mu^{(i,1)}(V)$, reducing them to combinations of scalar integrals. This decomposition can be performed automatically using a symbolic manipulation program, in our case FORM [19]. To make sure of the result, we checked it using a corrected and adapted version of a FORM program by J. Vermaseren based on the methods discussed in Ref. [20].

Having separated the tensor structure of the hadronic vertex from the scalar integrals, the next step is to write down the matrix element as a linear combination of a fundamental set of Lorentz structures involving spinors, polarization vectors, Dirac matrices and external momenta, with scalar coefficients. This is the method of standard matrix elements, described in detail in Ref. [21].

In the present case, after using momentum and current conservation, as well as the mass-shell conditions, the hadronic vertices $H_\mu^{(0,1)}(V)$ can be expressed as combinations of 4 standard matrix elements. The more complicated vertices $H_\mu^{(1,1)}(V)$, which carry two vector indices and depend on three momenta, can be expressed as linear combinations of 40 standard matrix elements. The coefficients of these linear combinations are deduced from the Passarino-Veltman procedure. In the algebraic manipulations which reduce $H_\mu^{(1,i)}(V)$ $(i = 0, 1)$ to standard matrix elements, $\gamma_5$ has

been assumed to anticommute with all $\gamma$ matrices. This is consistent in the present calculation, which contains no anomalous contributions. In particular, it can be seen that a naïve implementation of the method of standard matrix elements corresponds to the treatment of $\gamma_5$ suggested in Ref. [22]. The resulting decomposition into standard matrix elements multiplied by scalar form factors was automatically translated into FORTRAN code, to be readily implemented in a numerical evaluation of the square of the matrix element.

The final step is the evaluation of the scalar integrals, which is done analytically, using dimensional regularization both for ultraviolet and infrared divergences. The non-trivial integrals are four "triangle" integrals and one "box" integral, which can all be evaluated using standard methods. It should be noticed that for the present purposes it is important to keep the imaginary parts of the scalar integrals, since the $Z$ propagator has an imaginary part, and there will be real contributions to the square of the matrix element arising from the interference of the $Z$ width with the imaginary parts of the scalar integrals.

After renormalization, virtual corrections still contain infrared divergences, which must cancel against real soft gluon emission. The infared divergent part of the one-loop correction must be given by the well-known universal soft factor, multiplied by the tree-level contribution. This provides a first non-trivial analytic check of the algebraic manipulations performed on the matrix element. We have further tested the matrix element, computed numerically using our program, by verifying gauge invariance with respect to the external photon, and we have also tested the conservation of the vector current on the hadronic vertex in the case in which this conservation is not used in the construction of the standard matrix elements. A similar test for the axial current is non-trivial since we are working with massive quarks, so that the axial current is not conserved, but rather related by a Ward identity to pair production by a pseudoscalar source.

Real gluon emission corresponds to the process

$$e^-(p) + e^+(p') \to Q(p_1) + \bar{Q}(p_2) + \gamma(p_3) + g(p_4) \quad , \tag{7}$$

which admits a decomposition analogous to Eq. (3). The amplitude for this process is known, and for its evaluation we have used the codes described in Ref. [2]. In the soft gluon region, the amplitude factorizes as usual into the product of an eikonal factor times the tree-level amplitude for the process in Eq. (2). The resulting infrared divergent contribution to the cross section can easily be calculated analytically, and it cancels the corresponding divergence due to virtual gluon exchange, according to Eq. (1).

# 4 Results

In this paper we concentrate on the production of a photon in association with $b$ quarks at LEP1. We take $m_b = 4.7$ GeV, $\alpha_s = \alpha_s(M_Z) = 0.122$, $\alpha = 1/128.07$, $\sin^2\theta_W = 0.2247$, $M_Z = 91.187$ GeV, and $\Gamma_Z = 2.49$ GeV.

In Fig.1 we present the cross sections $\sigma_n = \sigma(\gamma + n\ jet)$ for the production of a photon plus $n$ jets, with $n = 1,\ 2,\ 3$, at leading order (LO) and including $\mathcal{O}(\alpha_s)$ corrections (NLO). The center–of–mass energy is set to $\sqrt{s} = M_Z$, and the cross sections are given as functions of $y_{cut}$, including both photon and $Z$ intermediate states, as well as the contribution of hard photon emission from the $e^+e^-$ pair. We neglect the effect of soft multiple initial state radiation. Events are accepted if the photon energy and transverse momentum are in the range

$$E_\gamma > 10\ \text{GeV} \qquad , \qquad p_\gamma^T > 5\ \text{GeV} \quad . \tag{8}$$

A minimum angle $\theta_{min} = 15^\circ$ is required between the photon and both quarks. For the real contribution, if the gluon is such that $m_{Qg}^2 > \Delta_0^2 = m_b^2 + 0.1 = 22.19$ GeV$^2$, the same minimum angle is required between the photon and the gluon. We have tested that our results are not sensitive to the particular choice of $\Delta_0$. In particular, varying the ratio $(\Delta_0^2 - m_b^2)/m_b^2$ by two orders of magnitude affects typical observables at the level of $1 - 2\%$.

Jets are reconstructed using the invariant mass squared of the parton pairs

$$y_{ij} = \frac{(p_i + p_j)^2}{s}. \tag{9}$$

However, our code is flexible and other jet reconstruction algorithms can be readily adopted. As we mentioned in section 2, the single parameter $y_{cut}$ is used both to define the number of jets in the event and to test the photon isolation from the jets, after reconstruction. With the present set of cuts the contribution of photon emission from the lepton pair amounts to about 5% of the total cross section.

In Fig. 2 we show the fractional change $R_i = (\sigma_i^{NLO} - \sigma_i^{LO})/\sigma_i^{LO}$ of NLO to LO cross section for $\sigma_1$ and $\sigma_2$. Finally, in Figs. 3, 4 and 5 we show a few examples of observable distributions that can be studied using the present calculation. Fig. 3 shows the photon energy distribution, Fig. 4 the transverse momentum one, while Fig. 5 deals with the cosine of the angle with respect to the $e^-$ direction. All distributions are given both at LO and at NLO, are obtained for $y_{cut} = 10^{-2}$, and are summed over the number of jets produced in association with the photon.

Notice that the cross section $\sigma_1$ is hardly modified by QCD corrections. In the $y_{cut}$ range we have examined $\sigma_1$ is always very small, at most of the order of 10%. The cross section $\sigma_3$ at $\mathcal{O}(\alpha_s)$ is completely determined by tree–level real emission diagrams and shows the usual steep rise for small values of the jet–jet separation parameter, which will eventually be tamed by the inclusion of $\mathcal{O}(\alpha_s^2)$ corrections. The most interesting result is the strong modification of the rate for two jets plus photon production. At large values of $y_{cut}$, $\sigma_2$ increases with respect to the LO result due to the contribution of three parton events in which two of the partons are unresolved. The growth of the cross section at smaller value of $y_{cut}$ is slower at NLO until, at about $y_{cut} = 2 \times 10^{-2}$, $\sigma_2$ begins to decrease quite sharply. At $y_{cut} = 1 \times 10^{-2}$, $\sigma_2 \approx \sigma_3$.

The size of NLO radiative corrections is illustrated in Fig.2. The corrections are relatively small for the one–jet case and positive. They are negligible at $y_{cut} = 1 \times 10^{-1}$ and increase for decreasing $y_{cut}$, reaching 30% at $y_{cut} = 1 \times 10^{-2}$. For the two–jet case they are negative for $y_{cut} < 5 \times 10^{-2}$ and positive for larger separations. The corrections are about –60% at $y_{cut} = 1 \times 10^{-2}$ and +30% at $y_{cut} = 1 \times 10^{-1}$, much like in the massless case, as shown for example in Ref. [12]. The corrections to $\sigma_1$ in the massive quark case have the opposite sign with respect to the massless quark result and are much smaller in magnitude.

The shapes of the differential distributions are not strongly affected by $\mathcal{O}(\alpha_s)$ corrections. The only modification of some interest is the kink at $E_\gamma \approx 22.5$ GeV in the photon energy spectrum. This kink can be traced back to the behaviour of the box diagrams, whose contribution is large and positive. Box diagrams correspond to a rescattering of the quark and antiquark after photon emission has taken place. As a consequence of this rescattering, high energy photons are less suppressed at one loop than at tree level, where the corresponding matrix element must contain a far off shell propagator. The differential $E_\gamma$ distribution of all remaining diagrams is smooth at all energies. These latter diagrams cancel to a large extent, resulting in a relatively small negative contribution. The presence and the location of the kink are insensitive to $E_{min}$, $p^T_{min}$, $\theta_{min}$ and to the quark mass. In fact we have checked that the same behaviour is reproduced for a $c$–quark with $m_c = 1.7$ GeV. On the other hand, varying the center–of–mass energy the location $E_k$ of the kink does change. In the range 80 GeV $< \sqrt{s} <$ 120 GeV we find $E_k \approx \sqrt{s}/4$. This effect is present even if in pure QED, namely if we only consider the contribution of the photon intermediate state neglecting the diagrams with a virtual $Z$. Given the limited statistics which can be expected, we are skeptical about the possibility of measuring the energy spectrum with enough accuracy to test for this kind of behaviour.

Notice finally that all the results are affected by an unphysical logarithmic dependence on the scale $\mu$ chosen for the running QCD coupling, as with all calculations that are of leading order in $\alpha_s$.

# 5 Conclusions

We have presented complete results for the $O(\alpha_s)$ corrections to the production of a heavy quark pair plus a hard photon, in $e^+e^-$ annihilation, including both photon and $Z$ intermediate states. Our results are implemented in a computer code that evaluates numerically the relevant matrix elements and combines them using a jet reconstruction algorithm to give the cross sections for hard photon production in association with $n$ jets, with $n = 1$, 2 and 3. The resulting fully differential cross sections can be used to construct arbitrary distributions, with the desired experimental cuts.

We have discussed in detail the production of a photon in association with $b$

quarks at LEP1, and we have given a few examples of relevant distributions in that case. We observe that the shape of the cross section for the production of 2 jets plus a resolved photon is significantly affected by NLO corrections, as may be expected, since the small-$y_{\rm cut}$ growth of the tree level result must be tamed by radiative corrections. The shapes of the other differential distributions is not significantly affected by radiative corrections. However it is possible to see the effects of the correlations between partons induced by gluon exchange, albeit at a level probably inaccessible experimentally. The overall normalization of the distributions is shifted downwards by QCD corrections, as may be expected, since virtual corrections are negative, while the inclusion of gluon radiation restricts the available phase space for hard photon emission, so that comparatively more photon events are excluded by the cuts.

The present work can be readily extended to other heavy quarks and higher energies, notably to the case of photon production in association with top pairs at future linear colliders. Work on these applications, as well as on a detailed comparison with the massless quark case, is in progress.

### Acknowledgements

We would like to thank Alessandro Ballestrero for many helpful discussions and for checking several parts of the computer code. L. M. would like to thank Dirk Kreimer for a helpful conversation, as well as Lance Dixon for his kind invitation to the Aspen Institute in the summer of 1995, where several discussions concerning the present work took place.

# References

[1] The LEP Electroweak Working Group, CERN/PPE/94–187, CERN/PPE/95–172.

[2] A. Ballestrero, E. Maina and S. Moretti, *Phys. Lett.* **B294** (1992) p. 425.
A. Ballestrero, E. Maina and S. Moretti, *Nucl. Phys.* **B 415** (1994) p. 265.

[3] A. Ballestrero and E. Maina, *Phys. Lett.* **B323** (1994) p. 53.

[4] J. Jersák, I. Laermann, and P.M. Zerwas, *Phys. Rev.* **D 25** (1982) p. 1218.

[5] G. Kramer and B. Lampe, *Phys. Lett.* **B 269** (1991) p. 401.

[6] R.K. Ellis, D.A. Ross and A.E. Terrano, *Nucl. Phys.* **B 178** (1981) p. 421.

[7] T. F. Walsh and P.M. Zerwas, *Phys. Lett.* **B 44** (1973) p. 195.
S.J. Brodsky, C.E. Carlson and R. Suaya, *Phys. Rev.* **D 14** (1976) p. 2264.
K. Koller, T.F. Walsh and P.M. Zerwas, *Z. Phys* **C 2** (1979) p. 2264.
E. Laermann, T.F. Walsh, I. Schmitt and P.M. Zerwas, *Nucl. Phys.* **B 207** (1982) p. 205.

[8] P. Mättig and W. Zeuner, *Z. Phys* **C 52** (1991) p. 37.

[9] R.N. Cahn, M.S. Chanowitz and N. Fleishon, *Phys. Lett.* **B 82** (1979) p. 113.
G. Gamberini, G.F. Giudice and G. Ridolfi, *Nucl. Phys.* **B 292** (1987) p. 237.

[10] A. Ali and C. Greub, *Z. Phys* **C 49** (1991) p. 431, and *Phys. Lett.* **B 259** (1991) p. 182.

[11] Z. Kunszt and Z. Trócsányi, *Nucl. Phys.* **B 394** (1993) p. 139.

[12] E.W.N. Glover and W.J. Stirling, *Phys. Lett.* **B295** (1992) p. 128.

[13] P. Mättig, H. Spiesberger and W. Zeuner, *Z. Phys.* **C 60** (1993) p. 613.

[14] ALEPH Coll., D. Buskulic *et al.*, *Z. Phys.* **C 57** (1993) p. 17.
DELPHI Coll., P. Abreu *et al.*, *Z. Phys.* **C 69** (1995) p. 1.
L3 Coll., M.Acciarri *et al.*, *Phys. Lett.* **B 346** (1995) p. 190.
OPAL Coll., R. Akers *et al.*, *Z. Phys.* **C 67** (1995) p. 15.

[15] E.L. Berger, X. Guo, J. Qiu, hep-ph/9512281.

[16] S.D. Ellis, Z. Kunszt and D.E. Soper, *Phys. Rev.* **D 40** (1989) p. 2188.
Z. Kunszt and D.E. Soper, *Phys. Rev.* **D 46** (1992) p. 192.
M.L. Mangano, P. Nason and G. Ridolfi, *Nucl. Phys.* **B 373** (1992) p. 295.

[17] W.T. Giele and E.W.N. Glover, *Phys. Rev.* **D 46** (1992) p. 1980.

[18] G. Passarino and M. Veltman, *Nucl. Phys.* **B 160** (1979) p. 151.

[19] J.A.M. Vermaseren, "FORM", Computer Algebra Nederland, Amsterdam 1991.

[20] G.J. van Oldenborgh and J.A.M. Vermaseren, *Z. Phys.* **C 46** (1990) p. 425.

[21] A. Denner, *Fort. Phys.* **41** (1993) p. 307.

[22] D. Kreimer, *Z. Phys.* **C 54** (1992) p. 503.

## Figure Captions

**Fig.1** Cross sections $\sigma_n = \sigma(\gamma + n\ jet)$ for the production of a photon plus $n$ jets, with $n = 1,\ 2,\ 3$, at LO and at NLO in QCD as functions of $y_{cut}$. Hard photon emission from the $e^+e^-$ pair is included. The jet reconstruction procedure and the set of cuts which ensure photon isolation are described in the text.

**Fig.2** Fractional difference $(\sigma_i^{NLO} - \sigma_i^{LO})/\sigma_i^{LO}$ for the production of a photon plus one and two jets as functions of $y_{cut}$.

**Fig.3** Photon energy spectrum at LO and at NLO in QCD for $y_{cut} = 1 \times 10^{-2}$. The separation parameter is $y_{ij} = (p_i + p_j)^2/s$.

**Fig.4** Tranverse momentum distribution of the photon at LO and at NLO in QCD for $y_{cut} = 1 \times 10^{-2}$.

**Fig.5** Distribution of the cosine of the angle between the photon and the incoming electron at LO and at NLO in QCD for $y_{cut} = 1 \times 10^{-2}$.

Fig.1

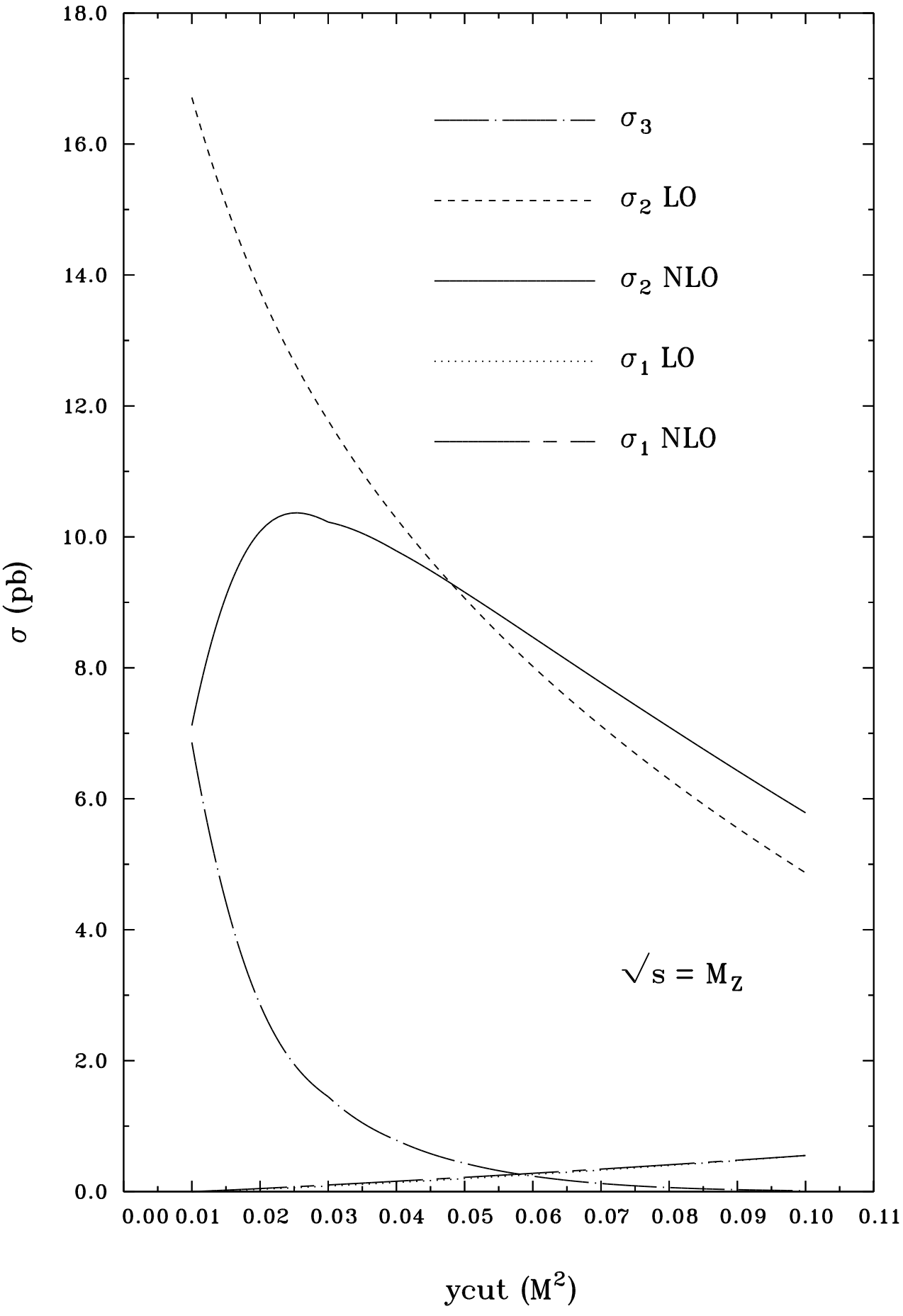
18.0
16.0
14.0
12.0
10.0
8.0
6.0
4.0
2.0
0.0
σ (pb)
0.00 0.01 0.02 0.03 0.04 0.05 0.06 0.07 0.08 0.09 0.10 0.11
ycut (M²)
σ3
σ2 LO
σ2 NLO
σ1 LO
σ1 NLO
√s = MZ

Fig.2

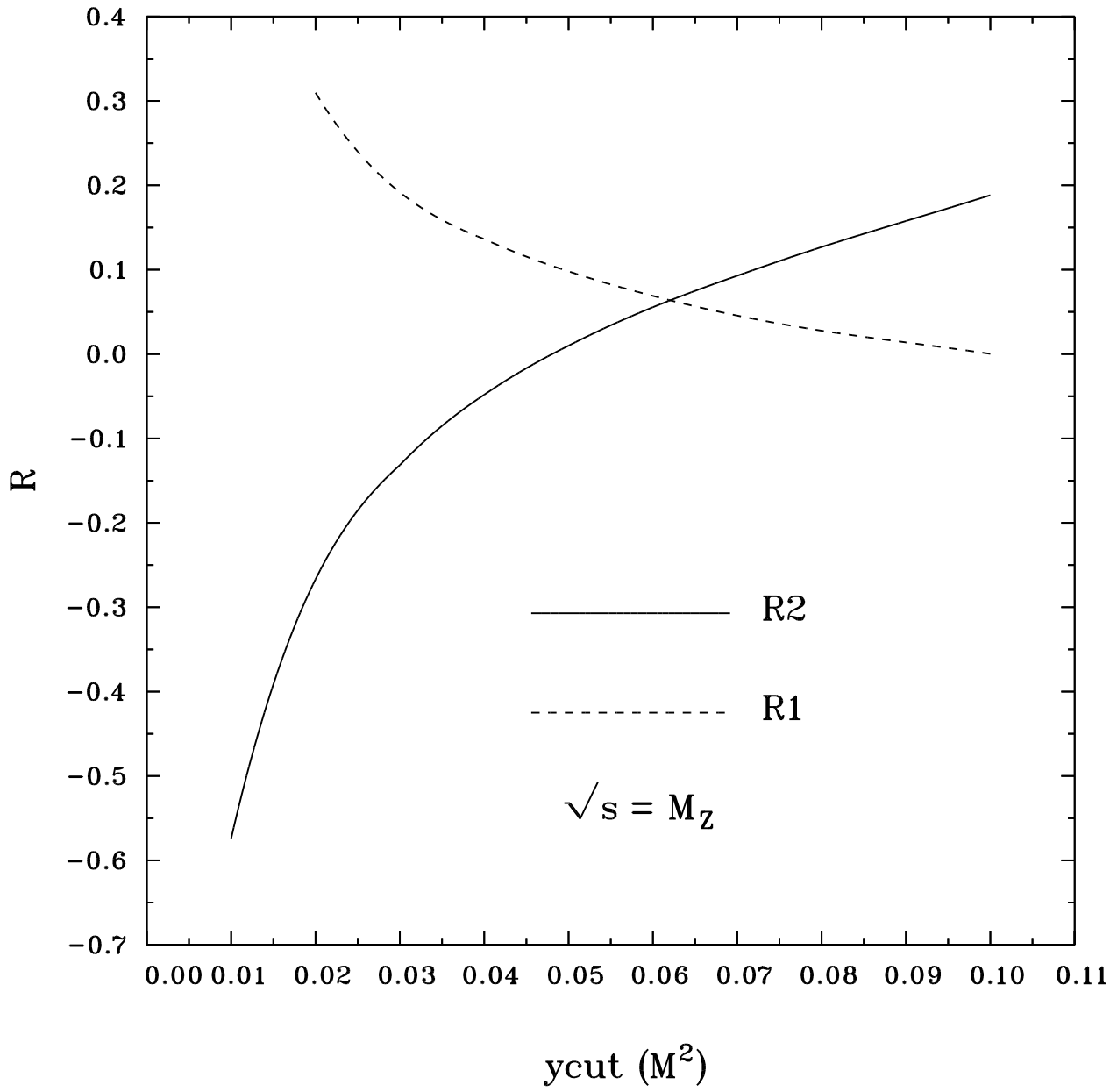
0.4
0.3
0.2
0.1
0.0
−0.1
−0.2
−0.3
−0.4
−0.5
−0.6
−0.7
R
0.00 0.01 0.02 0.03 0.04 0.05 0.06 0.07 0.08 0.09 0.10 0.11
ycut (M²)
R2
R1
√s = M_Z

Fig.3

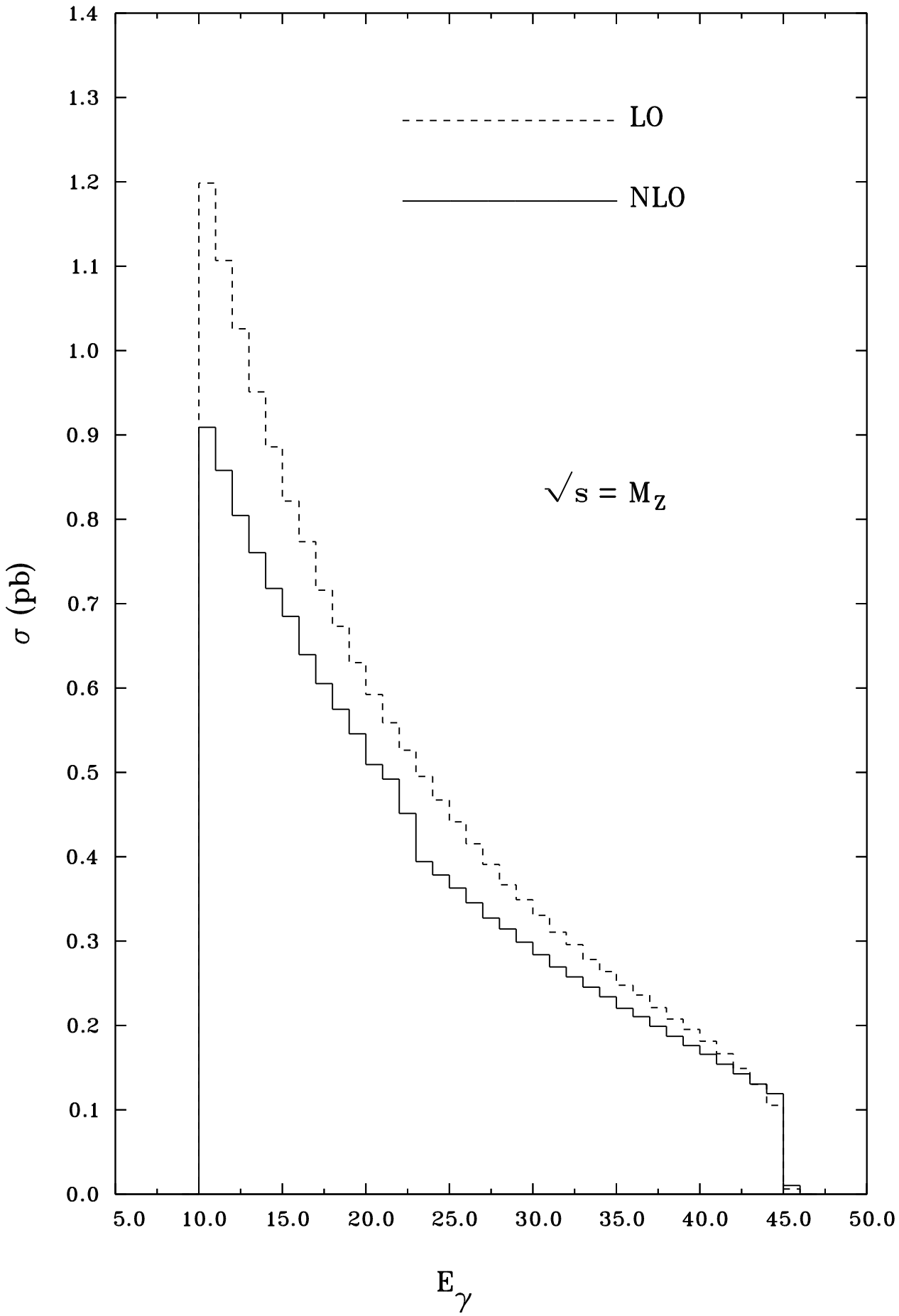
LO
NLO
$\sqrt{s} = M_Z$
σ (pb)
$E_\gamma$
1.4
1.3
1.2
1.1
1.0
0.9
0.8
0.7
0.6
0.5
0.4
0.3
0.2
0.1
0.0
5.0
10.0
15.0
20.0
25.0
30.0
35.0
40.0
45.0
50.0

Fig.4

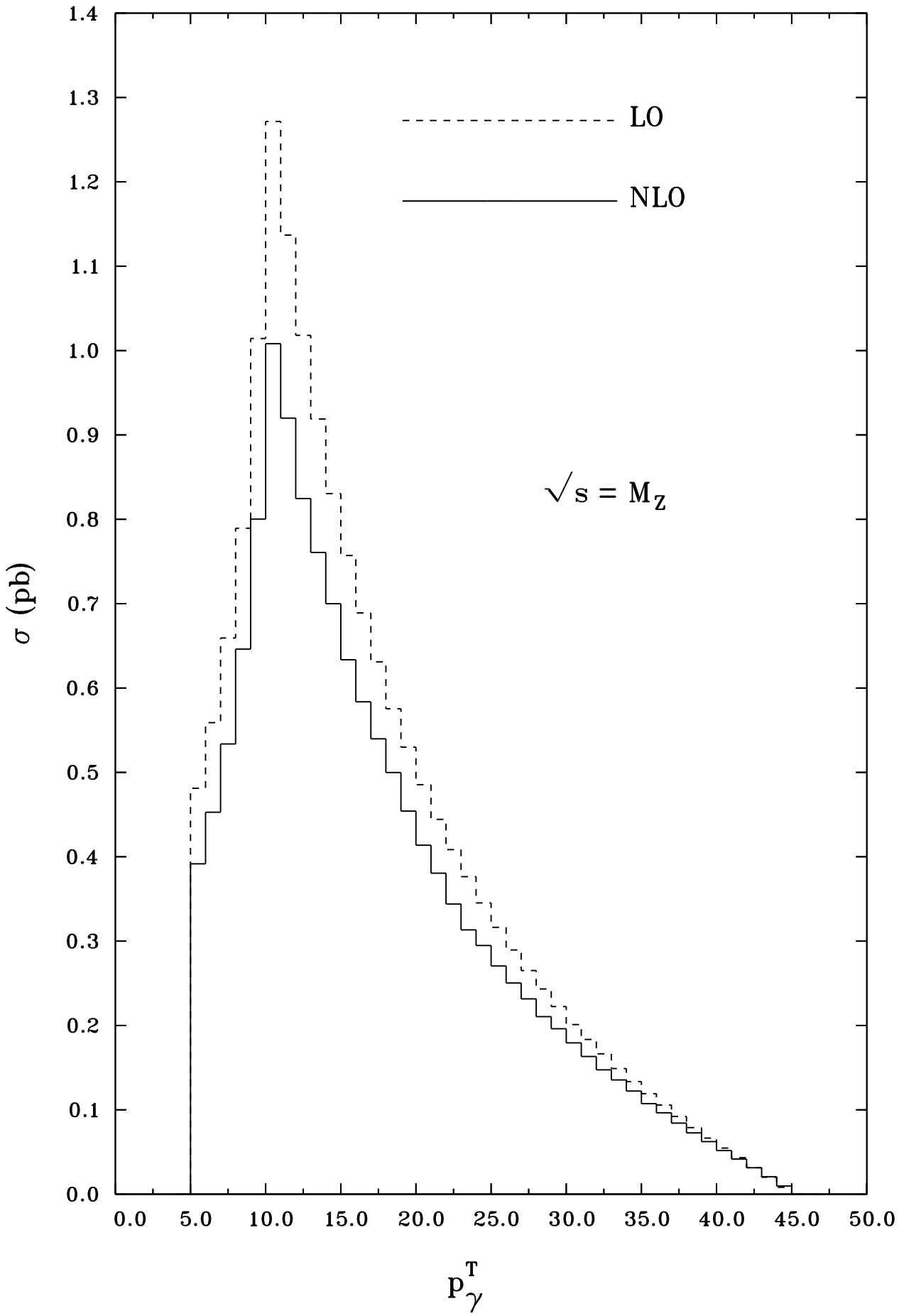
LO
NLO
$\sqrt{s} = M_Z$
$\sigma$ (pb)
$p_\gamma^T$
0.0
0.1
0.2
0.3
0.4
0.5
0.6
0.7
0.8
0.9
1.0
1.1
1.2
1.3
1.4
0.0
5.0
10.0
15.0
20.0
25.0
30.0
35.0
40.0
45.0
50.0

Fig.5

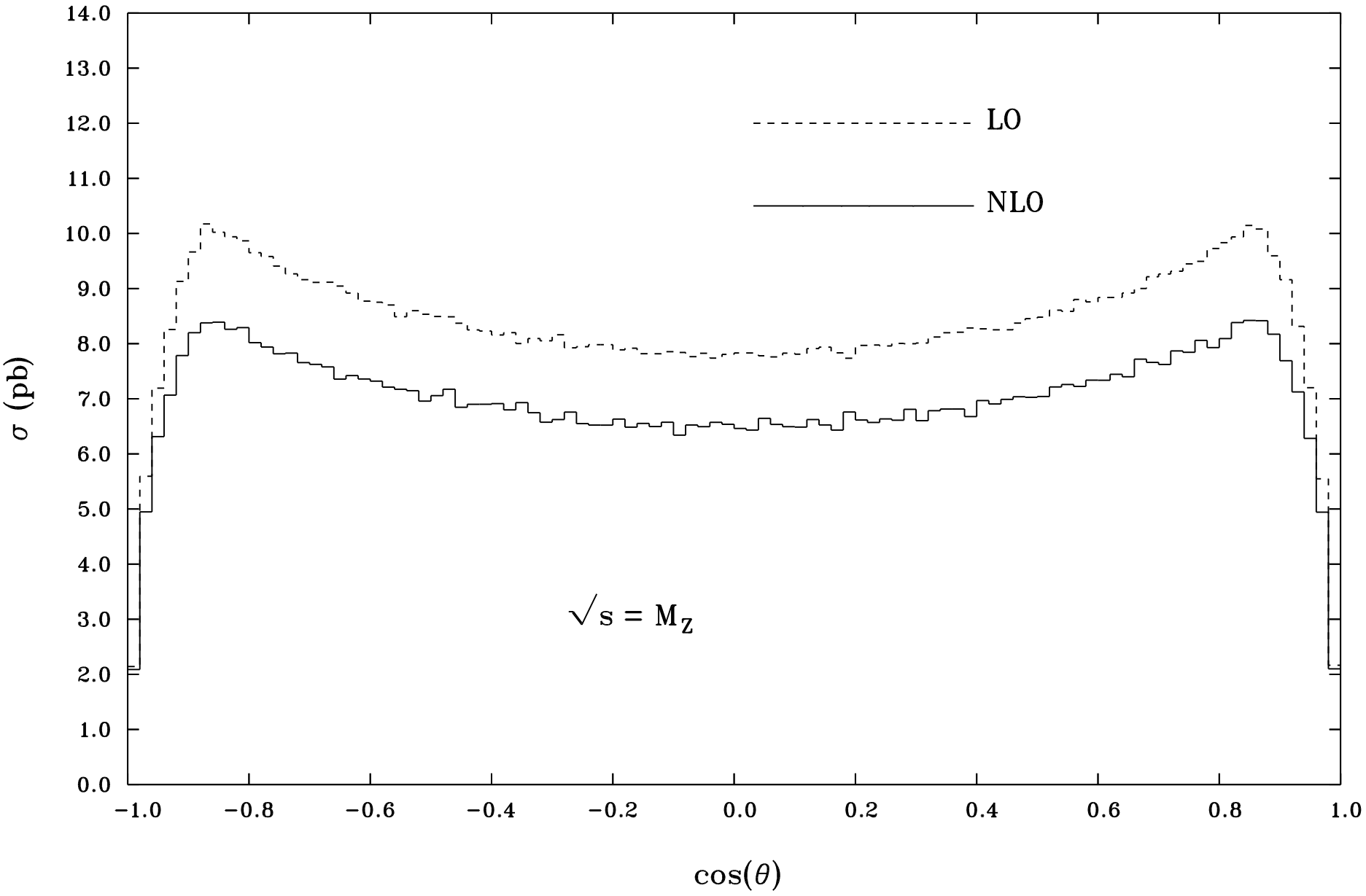
14.0
13.0
12.0
11.0
10.0
9.0
8.0
7.0
6.0
5.0
4.0
3.0
2.0
1.0
0.0
σ (pb)
LO
NLO
√s = M_Z
−1.0
−0.8
−0.6
−0.4
−0.2
0.0
0.2
0.4
0.6
0.8
1.0
cos(θ)